Anion transport properties of amine and amide-sidechained peptides are affected by charge and phospholipid composition†

Lei You,[a] Ruiqiong Li[a] and George W. Gokel*[a,b]

Received 11th January 2008, Accepted 16th April 2008
First published as an Advance Article on the web 16th June 2008
DOI: 10.1039/b800530c

Four synthetic anion transporters (SATs) having the general formula (n-$C_{18}H_{37}$)$_2$N-$COCH_2OCH_2CO$-(Gly)$_3$Pro-Lys(ε-N-R)-(Gly)$_2$-O-n-C_7H_{15} were prepared and studied. The group R was Cbz, H (TFA salt), *t*-Boc, and dansyl in peptides **1**, **2**, **3**, and **4** respectively. The glutamine analog (GGGPQAG sequence) was also included. A dansyl-substituted fluorescent SAT was used to probe peptide insertion; the dansyl sidechain resides in an environment near the bilayer's midpolar regime. When the lysine sidechain was free or protected amine, little effect was noted on final Cl^- transport rate in DOPC : DOPA (7 : 3) liposomes. This stands in contrast to the significant retardation of transport previously observed when a negative glutamate residue was present in the peptide sequence. It was also found that Cl^- release from liposomes depended on the phospholipid composition of the vesicles. Chloride transport diminished significantly for the free lysine containing SAT, **2**, when the lipid was altered from DOPC : DOPA to pure DOPC. Amide-sidechained SATs **1** and **5** showed a relatively small decrease in Cl^- transport. The effect of lipid composition on Cl^- transport was explained by differences in electrostatic interaction between amino acid sidechain and lipid headgroup, which was modeled by computation.

Introduction

Phospholipid membranes occur in astonishing variety even within organelles of the same cell.[1] Variations are found in all elements of the phospholipid monomer, including the hydrophobic tail(s), headgroup, *etc*. Common headgroups include choline, ethanolamine, serine, and inositol, among many others. These headgroups are typically linked through a phosphoryl residue to glycerol. Two fatty acids, esterified to primary and secondary glyceryl hydroxyl groups, generally provide the membrane's hydrophobic element.[2]

The great variability in phospholipid headgroups means that they may interact differently with their environment and/or with structures embedded within them.[3] Variations in the headgroup's charge state may alter the rate at which ions or molecules are transported through the bilayer. In recent studies conducted with hydraphile synthetic ion channels, we found that cation–π interactions involving phosphocholine headgroups[4] played a significant role in transport efficacy.[5] Further, organizational elements such as hydrogen bond donors or acceptors, residues that can participate in salt bridge formation, *etc.*, may exhibit unique interactions with certain membrane compositions.[6] It is known, for example, that many antibiotic peptides incorporate basic amino acids in their sequences, which enhance their affinity for Gram-negative bacteria, the outer membrane of which is negatively charged.[7–9]

A broad range of synthetic, membrane-active peptides has been developed in recent years. Examples include antibacterial peptides developed in the labs of Ghadiri[10] and Tirrell.[11] Pore-forming peptides have been reported by Voyer[12] and by Matile,[13] and their coworkers. At least the compounds reported by Ghadiri, Voyer, and Matile form pores that appear to disrupt cellular osmotic balance. Our non-peptidic hydraphile molecules do likewise.[14] Various synthetic non-peptide receptors, which can mediate anion transport through bilayer membrane, have also been designed, prepared and characterized.[15–19] We have prepared a family of pore-forming synthetic anion transporters (SATs) typically of the formula ($C_{18}H_{37}$)$_2$N-$COCH_2OCH_2CO$-(Gly)$_3$-Pro-(Gly)$_3$-OR.[20] Although not active as antibiotics against *E. coli*, they show chloride transport activity in vital mammalian cells. In the latter sense, they have potential as pharmaceutical agents.[21] The Cl^- transport efficacy of many members of this peptide family has been documented by studies involving liposomes[22] and at least 10-fold selectivity for chloride over potassium was observed by planar bilayer conductance measurements for the ∼(Gly)$_3$-Pro-(Gly)$_3$-$OC_{18}H_{37}$ derivative.[20,23] Both planar bilayer conductance studies and Hill plots comport with pore formation.[22,23]

In recent work, we systematically replaced each of the glycine residues in the sequence ∼(Gly)$_3$-Pro-(Gly)$_3$∼ on the *C*-terminal side of proline with glutamic acid.[24,25] The goal was to determine if the presence of a negatively charged residue within the pore formed by these compounds altered the Cl^- transport rate. A negative charge is, of course, expected to repel other negative charges, but this study sought to characterize the behavior of a pore formed within a phospholipid bilayer rather than in any bulk phase. The question was inspired by the proposal that a glutamic acid residue in the conductance pore of the ClC protein chloride transporter serves as a gate.[26,27] Indeed, the SAT containing a glutamate

[a]*Department of Chemistry, Washington University, St. Louis, MO 63130, USA*
[b]*Departments of Chemistry & Biochemistry and Biology, Center for Nanoscience, University of Missouri-Saint Louis, One University Boulevard, Saint Louis, MO 63121, USA. E-mail: gokelg@umsl.edu*

† Electronic supplementary information (ESI) available: Computational results. See DOI: 10.1039/b800530c

residue, was a measurably poorer Cl^- transporter than was the glutamate benzyl ester analog. In the present study, we pose two questions. First, does lysine, which should be protonated and positive within the conductance pore, affect Cl^- transport? Second, do variations in the membrane monomers and their charge balance affect Cl^- transport? In order to address these issues, we have developed a fluorescent probe, described below, that was used to gain insight into the function of SATs within the bilayer.

Results and discussion

Compounds studied

We have studied anion transport for numerous compounds of the type $(R^1)_2N\text{-}COCH_2OCH_2CO\text{-}(Gly)_3\text{-}Pro\text{-}(Gly)_3\text{-}OR^2$, in which R^1 ranged from methyl to octadecyl. The most common identity for R^1 was *n*-octadecyl. A number of derivatives were studied in which R^2 was varied, but in most examples R^2 was either benzyl or *n*-heptyl. The peptide sequences studied have been varied as well but were predominantly $(Gly)_3\text{-}Pro\text{-}(Gly)_3$.[28] Since most of the data were acquired with bis(octadecyl) derivatives, such as $(C_{18}H_{37})_2N\text{-}COCH_2OCH_2CO\text{-}(Gly)_3\text{-}Pro\text{-}(Gly)_3\text{-}OR^2$, and since transport activity was typically highest when R^2 was *n*-heptyl,[22] the compounds studied for the present report can be summarized as $(C_{18}H_{37})_2N\text{-}COCH_2OCH_2CO\text{-}(Gly)_3\text{-}Pro\text{-}Lyx\text{-}(Gly)_2\text{-}O(CH_2)_6CH_3$. The abbreviation Lyx is used to connote a lysine derivative having various substituents on the ε-amino group. The lysine derivatives **1**–**4** are illustrated, along with **5**, which has the structure $(C_{18}H_{37})_2N\text{-}COCH_2OCH_2CO\text{-}(Gly)_3\text{-}Pro\text{-}Gln\text{-}Ala\text{-}Gly\text{-}O(CH_2)_6CH_3$.

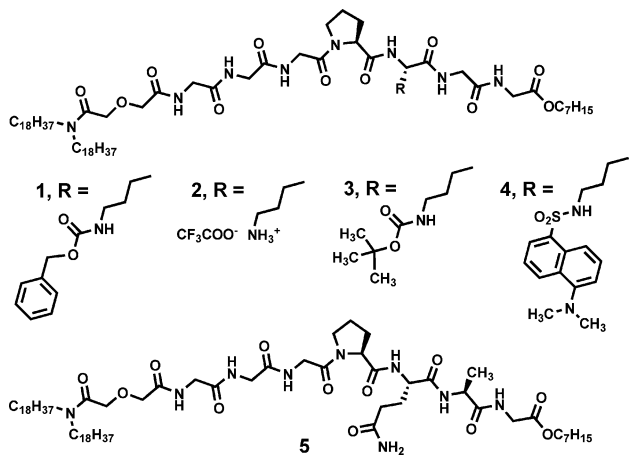

L-Lysine was incorporated in the fifth position of the sequence noted above to give ∼$(Gly)_3$-Pro-Lys-$(Gly)_2$∼ (∼GGGPKGG∼). The ε-amino group of lysine was functionalized as follows: **1**, benzyloxycarbonyl (Cbz); **2**, free amine, trifluoroacetic acid salt; **3**, *tert*-butoxycarbonyl (*t*-Boc); **4**, dansyl. This range of compounds permitted us to assess three issues. First, dansyl derivative **4** was used to determine if it, and by inference the lysine derivatives, inserts into the bilayer. Second, compound **2** places a positive charge (protonated amino group) within the conductance pore. Evidence obtained in previous studies suggests that the conductance pore forms from at least two monomers,[22] so two (or more) positive charges should be present. A third issue concerns the influence of changes in bilayer composition on the transport efficacy of these SATs. The results are described in the sections below.

Compound preparation

Standard solution coupling methods were used to prepare **1**–**5**. The ε-amino group of lysine was protected during peptide coupling. During the preparation of peptide **1**, Fmoc protected the main chain amino group and the sidechain amino group was masked by Cbz. The "orthogonal" protecting groups Cbz and Fmoc can be removed by hydrogenolysis or by treatment with base, respectively. The *C*-terminal, three amino acid sequence was prepared by coupling the lysine derivative with glycylglycine *n*-heptyl ester tosylate (EDCI, HOBt, NMM, CH_2Cl_2) to afford tripeptide Fmoc-(ε-N-Cbz)KGG-OC_7H_{15}. The Fmoc group was removed in the presence of Et_2NH. The free amine was then treated with Boc-proline to give Boc-P(ε-N-Cbz)KGG-OC_7H_{15}. After cleavage of the Boc group (HOAc : TFA, 3 : 7), the amine salt was coupled with previously reported[22] $(C_{18}H_{37})_2N\text{-}COCH_2OCH_2CO\text{-}(Gly)_3\text{-}OH$ to afford **1**. Compounds **2**–**5** were prepared by using a similar strategy. Synthetic access to **1** is summarized in Scheme 1 and details are recorded in the Experimental section.

Use of dansyl-SAT 4 as a fluorescent membrane probe

The dimethylaminonaphthylsulfonyl or dansyl group is highly fluorescent. It can readily be conjugated to the sidechain amino group of lysine to serve as a probe of amphiphile self-assembly and to probe insertion into the bilayer. Data are shown in Fig. 1 for chloride release mediated by **1**–**4** from vesicles prepared from 1,2-dioleoyl-*sn*-glycero-3-phosphocholine (DOPC) and 1,2-dioleoyl-*sn*-glycero-3-phosphate monosodium salt (DOPA, structures shown). Dansyl-SAT **4** shows essentially the same chloride release behavior as does **3**. Fig. 1 shows that **2** appears to form a pore faster than **1**, **3**, or **4** but **2**–**4** show similar Cl^- release profiles over the observation period. Compound **1** shows an unexpected

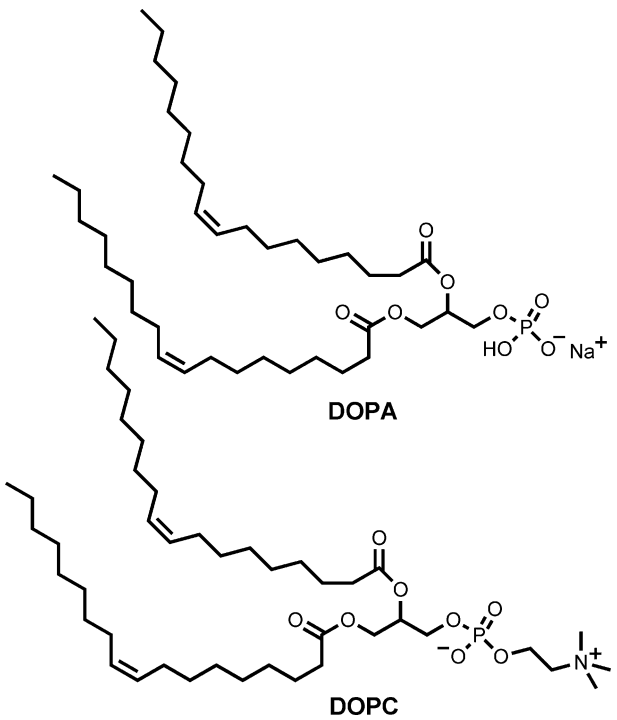

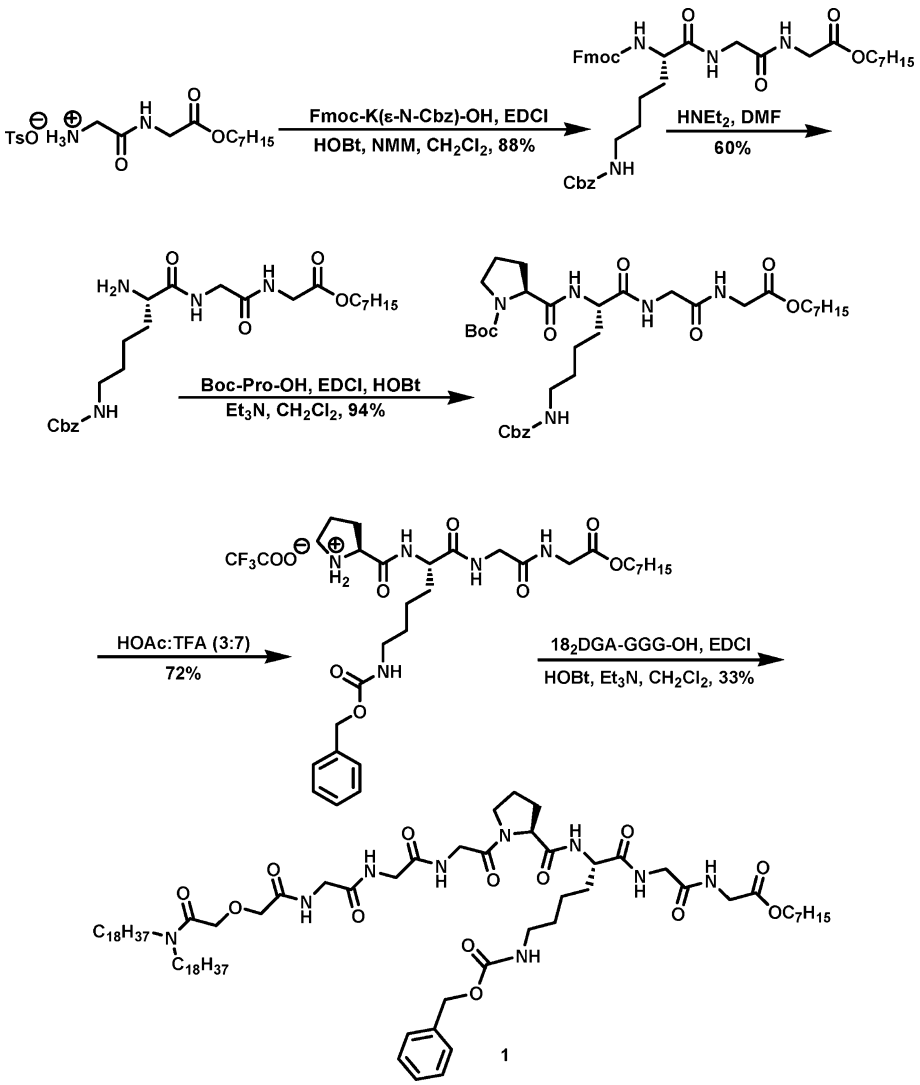

Scheme 1 Preparation of compound **1.**

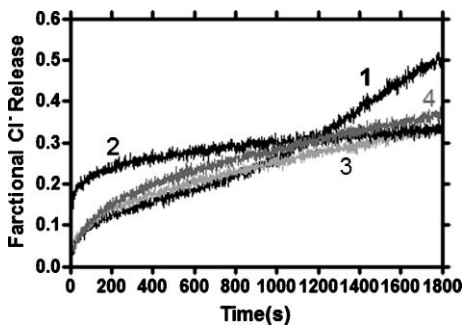

Fig. 1 Chloride release from DOPC : DOPA (7 : 3) liposomes mediated by **1**, **2**, **3**, and **4** (0.31 mM lipids, 65 μM compound, pH= 7.0).

increase in activity after about 1200 s. Although there are certainly differences in Cl^- release activity among these compounds, these data show that the fluorescent reporter in **4** does not fundamentally alter the peptide's behavior as is sometimes the case for fluorescent derivatives.

The fluorescence maximum (λ_{max}, λ_{exc} = 340 nm) was determined for **4** in solvents of varying polarity in order to better understand the dansyl group's position in the bilayer. This would, by inference, indicate the position of the lysine. Thus, the emission maximum for dansyl-SAT **4** was measured in hexane, dioxane, ethyl acetate, dichloromethane, 2-propanol, butanol, ethanol, and methanol (λ_{max} ~475–510 nm). The maxima were plotted on the ordinate *vs.* Reichardt's E_T polarity parameter (low to high values) on the abscissa.[29] The plot gave a straight line relationship (slope = 1.19, y intercept = 439.9 nm, r^2 = 0.97) over the range of solvents. The fluorescence maximum for **4** in DOPC : DOPA (7 : 3) liposomes was 492 nm. This corresponds to an E_T value of 43. Common solvents having similar E_T values are acetone, 42; dimethylformamide (DMF), 43; and butyrolactone, 44. It is clear that the dansyl group is neither exposed to the aqueous interface (high polarity) or embedded in the insulator/hydrocarbon regime (very low polarity) of the bilayer. This places dansyl at or near the midpolar (glyceryl) regime of the bilayer leaflet.[30] The fluorescence method does not permit greater precision in the present case because SAT insertion and pore formation are dynamic processes.

The fluorescence maximum (λ_{max}) observed for **4** suspended in HEPES buffer was 481 nm. Interpolation results in an E_T value of 35, which lies between hexane and dioxane on this scale. The aqueous buffer is very polar; the low polarity environment experienced by **4** shows that the amphiphilic peptide aggregates in aqueous solution, although the extent of this association is currently unknown.

Effect of membrane composition on the fluorescence spectrum of 4

In studies with hydraphile cation channels, we noted a significant effect of membrane composition on membrane transport. We have attributed this to cation–π interactions between the channel-former and the membrane monomer's headgroups.[5] We were thus interested to determine if the SAT pore-formers exhibited a membrane composition-dependent variation in anion transport. This was of particular significance in the present case as the positive charge of **2** could interact with the negatively charged phosphoryl residues in the membrane monomers.

The emission maximum of dansyl-SAT **4** was found to be 492 nm when it was recorded in vesicles prepared from a 7 : 3 (w/w) DOPC : DOPA mixture. Based on the polarity dependence study described above, the dansyl group of **4** should be near the midpolar/insulator (hydrocarbon) interface of the membrane in this monomer mixture. When liposomes were prepared from DOPC alone, an emission maximum was reproducibly observed at 490 nm for **4**, suggesting that dansyl resides in a slightly less polar environment than when present in DOPC : DOPA vesicles. Fig. 2 shows the variation in emission maximum (λ_{max}) in buffer, pure DOPC and the 7 : 3 DOPC : DOPA mixture. Based on these data and the polarity survey described above, the dansyl residue of **4** experiences diminishing polarity in the order DOPC : DOPA > DOPC > HEPES buffer.

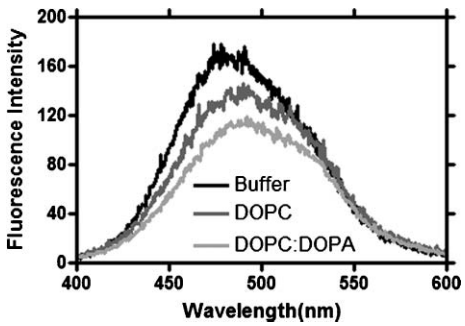

Fig. 2 The fluorescence emission spectra of **4** in aqueous buffer, DOPC, and DOPC : DOPA liposome suspension.

Chloride release mediated by compounds 1–4

The Cl^- release profiles of **1–4** in DOPC : DOPA liposomes are shown above in Fig. 1. The experiments were conducted as follows. The vesicles were loaded with 600 mM KCl in HEPES buffer (pH 7). The external buffer was chloride free, 400 mM K_2SO_4 in HEPES (pH 7). An Accumet chloride combination electrode was calibrated and the vesicle system was checked for leakage. With the electrode inserted into the aqueous liposome suspension, the ionophore under study was introduced (typically as a 2-propanol solution) and the electrode response was recorded during 0.5–1 h.

Typically, the chloride electrode showed ion release within seconds after ionophore addition. Automated data collection recorded an electrode potential every second. At the conclusion of an experiment, Triton X-100 detergent was added to lyse the vesicles and a final reading established $[Cl^-] = 100\%$. The release data were normalized to the final chloride concentration and are presented as fractional chloride release. Each data set is the average of at least three independent experiments.

Effect of lysine on chloride transport

One of the key questions we wished to address was whether or not protonated lysine affects Cl^- release from liposomes. Structurally, compounds **1–4** differ only by the presence or absence of the functional group on the lysine residue in the peptide's fifth (GGGPXGG) position. The sidechain amino group of lysine is reported to have a pK_A of 10.54, so it will be completely protonated at any pH below 8. Fig. 1 (above) shows that chloride release from DOPC : DOPA vesicles by **1–4** is generally similar, although ultimate release by **1** is greater and pore formation by **2** is faster than the others. Release of Cl^- by **1** before 1200 s is about the same as for **3–4** and only about 50% higher at 0.5 h. The reason for these two variations is obviously of interest but beyond the scope of the present work. The fluorescence results show that **4** aggregates in buffer so the dynamics of both insertion and pore formation could both differ somewhat for each of the structures.

The key finding here is that the positively charged lysine sidechain in **2** appears not to have a significant overall effect on the Cl^- transport rate, although the initial rate is somewhat faster. In previous work, we found that a similarly placed glutamate significantly diminished chloride transport under comparable conditions.[24,25] The effect of positive charge in or near the conductance pore is clearly less significant than is the presence of negative charge.

There are at least two explanations for the differences in charge effect. In one sense it is obvious that a negative charge (ionized glutamic acid) in a confined space should repel another negative charge and a positive charge (protonated lysine) should attract it. In the latter case, attraction of the anion may favor transport although too strong an interaction could diminish it. The lack of an observed effect may be due to offsetting effects.[31] Alternately, it may be that the amide residues of the GGGPXGG sequence bind[32,33] the carboxylate anion, partly blocking the pore or otherwise reorganizing it. The amides are less likely to interact with the ammonium ion although some H-bonding may occur there as well.

Effect of lipid composition on chloride transport

The second major question of the present study concerned the effect, if any, of lipid composition on the efficacy of Cl^- release mediated by **1–4**. Vesicles were prepared either from pure DOPC or 7 : 3 DOPC : DOPA as described above and Cl^- release was monitored. The headgroup of DOPA is negatively charged, whereas DOPC is overall neutral but is terminated by a trimethylammonium residue (see structures above). The results of Cl^- release from DOPC vesicles, mediated by **1–4**, are shown in Fig. 3. Protected sidechain amine derivatives **3** and **4** show behavior similar to that exhibited in DOPC : DOPA vesicles while **1** is

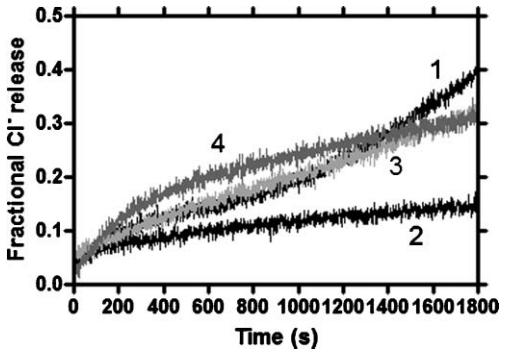

Fig. 3 Chloride release from DOPC liposomes mediated by **1**, **2**, **3**, and **4** (0.31 mM lipids, 65 μM compound, pH= 7.0).

slightly less active in DOPC vesicles. Positively charged **2**, however, was significantly less active in pure DOPC liposomes. The chloride release from DOPC mediated by glutamate containing SATs has similar result as that from DOPC : DOPA (7 : 3) liposomes.

Comparison of transport rates

It is clear from the data that transport by these synthetic anion transporters differs according to membrane composition. Since the release curves vary from DOPC : DOPA (7 : 3) to DOPC, especially from 0–200 s, we chose an arbitrary time point for comparison.[5] The fractional chloride release at 1500 s for each compound is summarized in Fig. 4. The left hand (open) bar is the transport rate for the compound in the 7 : 3 DOPC : DOPA mixture. The right hand (filled) bar is for an identical experiment conducted in DOPC only lipids. Each data set is the average of at least three independent measurements (error bars shown). Previously reported **5**, $(C_{18}H_{37})_2$N-$COCH_2OCH_2CO$-$(Gly)_3$-Pro-Gln-Ala-Gly-OC_7H_{15}, was used as a control compound since it contains a sidechain amide moiety, as do compounds **1** and **3**.

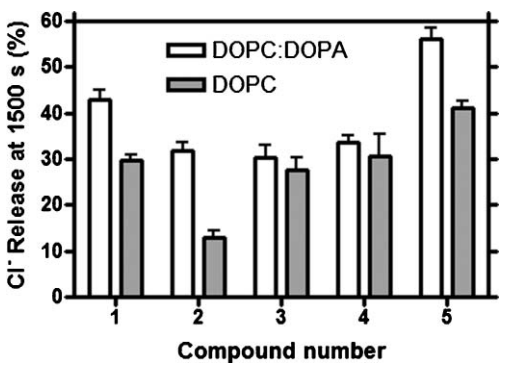

Fig. 4 Comparison of fractional chloride release at 1500 s mediated by **1–5** in DOPC or DOPC : DOPA liposomes.

The transport results for compounds **1–5** can be summarized in three groups. The Cl^- transport rates for **3** and **4** are unchanged within experimental error, irrespective of lipid composition. Compounds **1** and **5**, which have neutral but polar carbamate and amide sidechains, respectively, show about 70% of the transport activity in DOPC membranes compared to the DOPC : DOPA mixture. Lysine-containing **2** shows a drop in Cl^- transport ability to only 40% of its previous value. We note that both **1** and **3** incorporate carbamate residues in their sidechains, but the activity of the former is diminished and the latter is not. Our main focus here was to determine if there was lipid dependence on anion transport mediated by **2**. Such an effect was observed. The lipid effect on **1** remains unclear but it is only half that observed for **2**.

Compound **2**, which has a positively charged sidechain, is less active as a chloride transporter than either **1** or **5** at the arbitrarily chosen 1500 s time point. The Cl^- release mediated by **2** at 1500 s decreases by 60% when the lipid composition is changed. Since there was little change in the transport rate between protonated and neutral sidechained **2–4** in DOPC : DOPA (7 : 3) liposomes, we infer that there is a significant interaction between transporter **2** and lipid monomer. This interaction must be weaker for **3** and **4**. Possible interactions between a phospholipid headgroup and a SAT sidechain can involve H-bonding, salt bridge formation, charge–charge, or dipole–dipole interactions. Four plausible interactions are shown in Fig. 5.

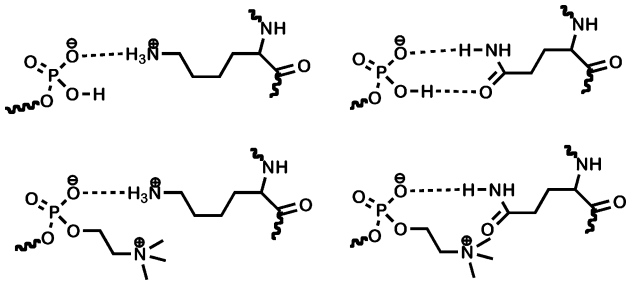

Fig. 5 Plausible interactions between phospholipid headgroup and ammonium (left) or amide residues (right).

Molecular modeling study

We applied computational methods to simplified models of both the lipids and the SAT in order to gain insight into these possible interactions and to assess geometrical constraints. Such calculations could be done on an ensemble of lipid monomers[34] and SAT molecules. Such calculations require a huge amount of CPU time even with the most capable processors. We thus simplified the system as follows. The phospholipids were modeled as methyl phosphate. DOPA was modeled as dimethylphosphate monosodium salt while DOPC was modeled as dimethylphosphocholine. The isolated *N*-terminus of lysine or glutamine was capped with an acetyl group to mimic an amide residue. The peptide's *C*-terminus was simplified as a methyl ketone to minimize the number of additional H-bond donor and acceptor interactions. We note that when more laborious calculations were done on a compound in which the *C*-terminus was a methyl ester rather than a methyl ketone, similar results were obtained.

The DFT method of Gaussian 03 was used to optimize geometries and to minimize energies (see Experimental section). Selected results are shown in Fig. 6. The calculations reported here were conducted for the gas phase. The limitations of a gas phase calculation are obvious but the dynamics of a membrane and the uncertain water content make simple alternatives untenable. Moreover, the structural information thus obtained will be internally comparable.

Bearing in mind the caveats noted above concerning both the gas phase and the choice of models and the tendency to over-interpret models, certain differences are apparent. The model for the

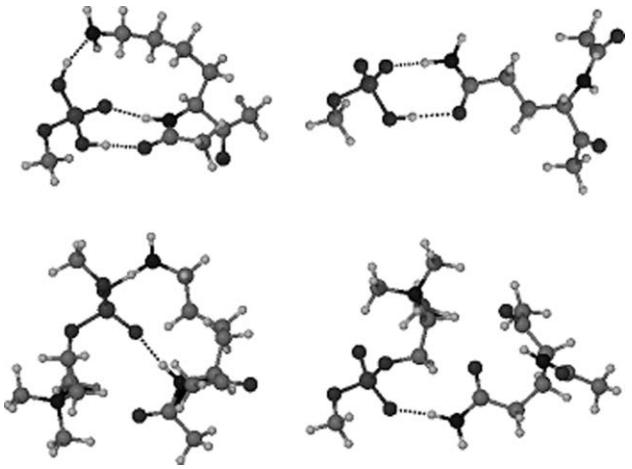

Fig. 6 Calculation results for four model complexes: phosphate–lysine (upper left), phosphocholine–lysine (lower left), phosphate–glutamine (upper right) and phosphocholine–glutamine (lower right).

lipid–ammonium sidechain interaction of **2** shows two or three H-bond associations (shown as dotted lines, left panels). The amide–lipid association that models the amide sidechain of **5** shows one or two such contacts (right panels). The calculated bond distances are recorded in the Supplementary Material†. The key issue here is that greater changes are predicted when **2** or **5** interacts with phosphate (DOPA model) than with phosphocholine (DOPC model). The calculations show that the interaction between phosphate and either the lysine or glutamine sidechain is more favorable than the corresponding phosphocholine interaction. These interactions may stabilize the active conformation of pore-formers more in DOPC : DOPA liposomes than in pure DOPC. Simplified as these models are, they comport with the transport data and with the suggestion offered above of differences in H-bond interactions within the pore.

Conclusion

Three important findings emerge from the present study. First, a positively charged residue (ammonium cation) within the chloride transporting pore does not favor final chloride transport rate through the bilayer mediated by the SAT molecules described here. Indeed, in the DOPC : DOPA (7 : 3) lipid system, the ammonium-sidechained SAT and those having a protected amine function exhibit similar activity. This result is strikingly different from the previously reported inhibitory influence of a negatively charged sidechain.[24,25]

A fluorescent dansyl residue was incorporated into the peptide sequence to probe the SAT's position in the bilayer. Dansyl fluorescence is solvent dependent and a correlation line between solvent polarity and fluorescence emission maxima was used to estimate the environment experienced by the fluorophore. In aqueous buffer, the amphiphilic peptide SATs aggregate. After insertion into the membrane, however, the emission is red shifted and the dansyl sidechain resides in an environment near the bilayer's midpolar regime.

The chloride transporting activity of amine- and amide-sidechained SATs is dependent on the liposome's phospholipid composition. The Cl^- transport ability of **2** decreases significantly when the lipid composition is changed from DOPC : DOPA to pure DOPC. This activity decrease is explained by differences in hydrogen bond interactions between the lipid phosphoryl group and the sidechain ammonium ion. Computational results using model systems showed that a phosphate–lysine interaction is stronger than a phosphocholine–lysine interaction. This is not surprising and it is known that basic amino acids show enhanced affinity for Gram-negative bacteria, the outer membrane of which is negatively charged.[7–9]

The Cl^- transport activity of sidechain amide containing compounds **1** and **5** also decreased when the DOPC : DOPA lipid composition was changed to DOPC. The effect is not as pronounced as that observed for amine derivative **2**, but this sidechain amide effect is notable because it is less well documented. The formation of a doubly bridged hydrogen bond interaction between amide and phosphate may play an important role that is supported by the computational models reported here.

Experimental section

General

^{1}H-NMR spectra were recorded on a Gemini 300 spectrometer and are reported in the following manner: chemical shifts reported in ppm (δ) downfield from internal $(CH_3)_4Si$ (integrated intensity, multiplicity (b = broad, s = singlet, d = doublet, t = triplet, q = quartet, bs = broad singlet, m = multiplet, *etc.*), coupling constants in Hz, assignment). ^{13}C-NMR spectra were obtained at 75 MHz and referenced to $CDCl_3$ (77.23 ppm). NMR spectra were obtained in $CDCl_3$ unless otherwise specified. Infrared spectra were recorded on a Perkin-Elmer 1710 Fourier transform infrared spectrometer. Melting points were determined on a Thomas Hoover apparatus in open capillaries and are uncorrected for crystalline compounds. Thin layer chromatography analyses were performed on silica gel 60-F-254 with a 0.2 mm thickness. Preparative chromatography columns were packed with silica gel (Kieselgel 60, 70–230 mesh or Merck grade 9385, 230–400 mesh, 60 Å).

Reagents were of the best grade commercially available and were distilled, recrystallized, or used without further purification, as appropriate. CH_2Cl_2 was distilled from calcium hydride. EDCI represents 1-(3-dimethylaminopropyl)-3-ethyl carbodiimide hydrochloride. HOBt represents 1-hydroxybenzotriazole. DMAP represents 4-dimethylaminopyridine. DGA represents diglycolyl, $\sim COCH_2OCH_2CO\sim$. Combustion analyses were performed by M-H-W Laboratories, Phoenix, AZ, and are reported as percents. High resolution mass spectra were obtained from the University of Missouri-Saint Louis mass spectrometry facility.

Preparation of $(C_{18}H_{37})_2NCOCH_2OCH_2CO$-$(Gly)_3$-Pro-Lys(ε-N-Cbz)-$(Gly)_2$-$OC_7H_{15}$, 1

Fmoc-K(ε-N-Cbz)GG-OC_7H_{15}. $TsOH{\cdot}GG\text{-}OC_7H_{15}$ (0.60 g, 1.49 mmol), Fmoc-K(ε- N-Cbz)-OH (0.75 g, 1.49 mmol), EDCI (0.31 g, 1.64 mmol) and HOBt (0.22 g, 1.64 mmol) were dissolved in CH_2Cl_2 (35 mL). NMM (0.18 mL) was added. The mixture was stirred at 0 °C for 0.5 h and then at room temperature for 24 h. The solvent was removed *in vacuo*. The residue was dissolved in CH_2Cl_2 (50 mL), washed with 5% citric acid (2 × 25 mL),

H_2O (2 × 25 mL), 5% $NaHCO_3$ (25 mL) and brine (25 mL), dried over $MgSO_4$ and evaporated. Column chromatography (silica gel, $CHCl_3$: CH_3OH = 98 : 2) afforded a white solid (0.94 g, 88%). ^{1}H-NMR: 0.87 (3H, t, J = 6.8 Hz, CH_2CH_3), 1.26 (8H, pseudo-s, $OCH_2CH_2(CH_2)_4CH_3$), 1.34–1.62 (6H, m, Lys $CH_2CH_2CH_2CH_2NH$ and $OCH_2CH_2(CH_2)_4CH_3$), 1.62–1.93 (2H, m, Lys $CH_2CH_2CH_2CH_2NH$), 3.17 (2H, d, J = 4.8 Hz, Lys $CH_2CH_2CH_2CH_2NH$), 3.96 (4H, d, J = 5.1 Hz, two Gly CH_2), 4.04 (2H, t, J = 6.9 Hz, $OCH_2CH_2(CH_2)_4CH_3$), 4.08–4.20 (2H, m, Lys *CH* and Fmoc *CH*), 4.39 (2H, d, J = 6.6 Hz, Fmoc CH_2), 5.06 (2H, s, OCH_2Ph), 5.10 (1H, bt, CO*NH*), 5.86 (1H, bd, CO*NH*), 6.96–7.07 (2H, m, two CO*NH*), 7.21–7.40 (9H, m, Ph H_{Ar} and Fmoc H_{Ar}), 7.51–7.60 (2H, m, Fmoc H_{Ar}), 7.74 (2H, d, J = 7.5 Hz, Fmoc H_{Ar}). ^{13}C-NMR: 14.2, 22.5, 22.8, 25.9, 28.6, 29.0, 29.6, 31.9, 40.3, 41.4, 43.1, 47.3, 55.4, 65.9, 66.8, 67.3, 120.2, 125.2, 127.3, 128.0, 128.3, 128.7, 136.8, 141.5, 143.9, 157.0, 169.2, 170.0, 172.7. IR ($CHCl_3$, cm^{-1}): 3301, 3066, 2931, 2858, 1739, 1689, 1645, 1537, 1451, 1406, 1263, 1134, 1104, 1090, 1032.

H_2N-K(ε-N-Cbz)GG-OC_7H_{15}. Fmoc-K(ε-N-Cbz)GG-OC_7H_{15} (0.83 g, 1.16 mmol) was dissolved in DMF (10 mL). Et_2NH (1.2 mL) was added and the reaction was stirred at rt for 2 h. The reaction was quenched by water (3 × 25 mL) and extracted with CH_2Cl_2 (3 × 25 mL). Organic layers were combined and washed with 5% $NaHCO_3$ (2 × 25 mL) and brine (2 × 25 mL). Dry over $MgSO_4$. The solvent was evaporated *in vacuo* and the residue was triturated with ether. Vacuum filtration afforded a white solid (0.32 g, 60%). ^{1}H-NMR: 0.89 (3H, t, J = 6.8 Hz, CH_2CH_3), 1.28 (8H, *pseudo*-s, $OCH_2CH_2(CH_2)_4CH_3$), 1.40–1.93 (8H, $OCH_2CH_2(CH_2)_4CH_3$ and Lys $CH_2CH_2CH_2CH_2NH$), 3.10–3.23 (2H, m, $CH_2CH_2CH_2CH_2NH$), 3.67 (1H, bs, *NH*), 3.85–4.17 (7H, m, two Gly CH_2, Lys *CH* and $OCH_2CH_2(CH_2)_4CH_3$), 5.08 (2H, s, OCH_2Ph), 5.21 (1H, bt, *NH*), 7.07 (1H, bs, *NH*), 7.27–7.40 (6H, m, Ph H_{Ar} and *NH*), 8.11 (1H, bs, *NH*). ^{13}C-NMR: 14.2, 22.5, 22.8, 26.0, 28.7, 29.1, 29.7, 31.9, 40.8, 41.4, 43.9, 66.0, 128.3, 128.7, 137.0, 169.6. IR ($CHCl_3$, cm^{-1}): 3318, 3067, 2929, 2858, 1742, 1690, 1657, 1542, 1455, 1411, 1370, 1260, 1212, 1137, 1028, 913.

Boc-PK(ε-N-Cbz)GG-OC_7H_{15}. H_2N-(ε-N-Cbz)KGG-OC_7H_{15} (0.32 g, 0.65 mmol), Boc-Pro-OH (0.14 g, 0.65 mmol), EDCI (0.14 g, 0.71 mmol) and HOBt (0.10 g, 0.71 mmol) were dissolved in CH_2Cl_2 (25 mL). Et_3N (0.27 mL) was then added. The mixture was stirred at 0 °C for 0.5 h and then at rt for 48 h. The solvent was evaporated and the residue was chromatographed (silica gel, $CHCl_3$: CH_3OH 98 : 2–97 : 3) to afford a yellow oil (0.42 g, 94%). ^{1}H-NMR: 0.88 (3H, t, J = 6.8 Hz, CH_2CH_3), 1.19–1.37 (8H, m, $OCH_2CH_2(CH_2)_4CH_3$), 1.44 (9H, s, $C(CH_3)_3$), 1.48–2.23 (12H, m, $OCH_2CH_2(CH_2)_4CH_3$, Lys $CH_2CH_2CH_2CH_2NH$ and Pro $NCH_2CH_2CH_2$), 3.18 (2H, bt, Lys $CH_2CH_2CH_2CH_2NH$), 3.34–3.51 (2H, m, Pro$NCH_2CH_2CH_2$), 3.88–4.06 (4H, m, two Gly CH_2), 4.11 (2H, t, J = 6.9 Hz, $OCH_2CH_2(CH_2)_4CH_3$), 4.16–4.38 (2H, m, Pro *CH* and Lys *CH*), 5.00–5.18 (3H, m, OCH_2Ph and *NH*), 7.00 (1H, bs, *NH*), 7.09 (1H, bs, *NH*), 7.28–7.38 (5H, m, Ph H_{Ar}), 7.46 (1H, bs, *NH*). ^{13}C-NMR: 14.2, 22.8, 22.9, 26.0, 28.6, 28.7, 29.1, 29.6, 31.9, 37.5, 41.4, 43.3, 47.5, 58.8, 60.9, 65.8, 66.8, 77.4, 83.9, 128.2, 128.3, 128.7, 136.9, 161.2, 170.0, 170.9, 173.4. IR ($CHCl_3$, cm^{-1}): 3309, 3068, 2931, 2860, 1748, 1674, 1535, 1455, 1404, 1367, 1250, 1204, 1164, 1128, 1090, 1029.

CF_3COOH·P(ε-N-Cbz)KGG-OC_7H_{15}. Boc-P(ε-N-Cbz)KGG-OC_7H_{15} (0.42 g, 0.61 mmol) was dissolved in HOAc (1.5 mL). The solution was cooled in ice and TFA (3.5 mL) was added. The mixture was stirred at rt for 50 min. The acids were rapidly removed *in vacuo* and the residue was triturated with ether. Vacuum filtration afforded a white solid (0.31 g, 72%). ^{1}H-NMR: 0.88 (3H, t, J = 6.9 Hz, CH_2CH_3), 1.20–1.45 (8H, m, $OCH_2CH_2(CH_2)_4CH_3$), 1.50–2.21 (12H, m, $OCH_2CH_2(CH_2)_4CH_3$, Lys $CH_2CH_2CH_2CH_2NH$ and Pro $NCH_2CH_2CH_2$), 3.14 (2H, bs, Lys $CH_2CH_2CH_2CH_2NH$), 3.43 (2H, bs, Pro $NCH_2CH_2CH_2$), 3.60–4.30 (8H, m, two Gly CH_2, $OCH_2CH_2(CH_2)_4CH_3$, Pro *CH* and Lys *CH*), 4.93 (2H, s, OCH_2Ph), 5.15 (1H, bs, *NH*), 6.20 (1H, bs, *NH*), 7.16 (5H, *pseudo*-s, Ph H_{Ar}), 7.35 (1H, s, *NH*), 8.20 (1H, bs, *NH*), 9.17 (1H, bs, *NH*), 11.53 (1H, bs, *NH*). ^{13}C-NMR: 14.2, 14.6, 22.8, 22.9, 25.9, 26.1, 28.7, 29.1, 29.3, 31.9, 36.2, 41.4, 43.3, 65.8, 74.6, 89.6, 128.2, 128.6, 160.2, 170.0, 206.5. IR ($CHCl_3$, cm^{-1}): 3320, 3069, 2932, 2860, 1743, 1671, 1546, 1455, 1410, 1369, 1256, 1204, 1136, 1029.

18_2DGA-GGGPK(ε-N-Cbz)GG-OC_7H_{15}, 1. 18_2DGA-GGG-OH (0.36 g, 0.44 mmol), CF_3COOH.PK(ε-N-Cbz)GG-OC_7H_{15} (0.31 g, 0.44 mmol), EDCI (0.093 g, 0.48 mmol) and HOBt (0.065 g, 0.48 mmol) were suspended in CH_2Cl_2 (20 mL). Et_3N (0.18 mL) was then added. The mixture was stirred at 0 °C for 0.5 h and then at room temperature for 48 h. The solvent was evaporated and the residue was crystallized from MeOH. The crude product was chromatographed (silica gel, $CHCl_3$: MeOH 95 : 5). Recrystallization from MeOH afforded a white solid (204 mg, 33%). ^{1}H-NMR ($CDCl_3$, almost all of the peaks are quite broad): 0.88 (3H, t, J = 6.6 Hz, CH_2CH_3), 1.20–1.70 (74H, m, $OCH_2CH_2(CH_2)_4CH_3$, $CH_3(CH_2)_{15}CH_2CH_2N$, $OCH_2CH_2(CH_2)_4CH_3$ and $CH_3(CH_2)_{15}CH_2CH_2N$), 1.70–2.30 (10H, m, Pro $NCH_2CH_2CH_2$ and Lys $(CH_2)_3CH_2NH$), 3.00–3.46 (8H, m, $CH_3(CH_2)_{15}CH_2CH_2N$, Lys $(CH_2)_3CH_2NH$ and Pro $NCH_2CH_2CH_2$), 3.60–4.44 (18H, m, Gly CH_2, $OCH_2CH_2(CH_2)_4CH_3$, $COCH_2O$, Pro *CH*, and Lys *CH*), 5.00–5.13 (2H, m, OCH_2Ph), 5.53 (1H, bs, *NH*), 7.30–7.40 (5H, m, Ph H_{Ar}), 7.53 (2H, bs, *NH*), 7.86 (2H, bs, *NH*), 8.64 (1H, bs, *NH*). ^{13}C-NMR: 14.2, 14.3, 22.8, 22.9, 23.1, 25.1, 26.0, 27.1, 27.3, 27.8, 28.7, 29.0, 29.1, 29.5, 29.6, 29.7, 29.8, 29.9, 31.9, 32.1, 40.4, 41.5, 42.7, 43.0, 43.4, 46.6, 47.2, 47.6, 54.0, 61.8, 65.8, 66.7, 69.8, 71.9, 128.2, 128.3, 128.7, 137.0, 156.8, 168.7, 169.8, 170.1, 170.3, 170.6, 171.6, 171.8, 172.5, 173.1. IR ($CHCl_3$, cm^{-1}): 3306, 3069, 2920, 2851, 1743, 1647, 1540, 1467, 1411, 1377, 1338, 1250, 1208, 1130, 1029. Anal. calcd for $C_{76}H_{133}N_9O_{13}$: C, 66.10; H, 9.71; N, 9.13%. Found: C, 66.04; H, 9.87; N, 9.15%.

Preparation of $(C_{18}H_{37})_2NCOCH_2OCH_2CO$-$(Gly)_3$-Pro-Lys-$(Gly)_2$-$OC_7H_{15}$·TFA, 2

18_2DGA-GGGPKGG-OC_7H_{15}·TFA, 2. 18_2DGA-GGGPK(ε-N-Boc)GG-OC_7H_{15}, **3** (64 mg, 0.048 mmol) was dissolved in CH_2Cl_2 (2 mL). TFA (2 mL) was then added. The mixture was stirred at room temperature for 2 h. Solvents were removed *in vacuo.* Toluene was added and the mixture evaporated to remove residual acid. High vacuum drying overnight afforded a white waxy solid (60 mg, 93%). ^{1}H-NMR ($CDCl_3$, all peaks are broad): 0.88 (9H, t, J = 6.5 Hz, CH_2CH_3), 1.20–2.30 (84H, m, $NCH_2CH_2(CH_2)_{15}CH_3$,

$OCH_2CH_2(CH_2)_4CH_3$, $NCH_2CH_2(CH_2)_{15}CH_3$, OCH_2CH_2-$(CH_2)_4CH_3$, Lys $CH_2CH_2CH_2CH_2NH$ and Pro NCH_2CH_2-CH_2), 2.80–3.20 (4H, m, $NCH_2CH_2(CH_2)_{15}CH_3$ and Lys $CH_2CH_2CH_2CH_2NH$), 3.26 (2H, bt, $NCH_2CH_2(CH_2)_{15}CH_3$), 3.44–3.78 (2H, m, Pro $NCH_2CH_2CH_2$), 3.80–4.20 (15H, m, Gly CH_2, $OCH_2CH_2(CH_2)_4CH_3$, Pro *CH* and OCH_2CO), 4.26–4.47 (3H, m, OCH_2CO and Lys *CH*), 7.71 (1H, bs, *NH*), 7.86 (4H, bs, *NH*), 8.14 (2H, bs, *NH*), 8.29 (1H, bs, *NH*), 8.44 (1H, bs, *NH*). ^{13}C-NMR: 14.2, 14.3, 22.8, 22.9, 25.2, 26.0, 26.6, 27.1, 27.3, 27.8, 28.7, 29.0, 29.1, 29.5, 29.6, 29.8, 29.9, 31.9, 32.1, 39.9, 41.4, 42.4, 42.9, 43.1, 46.0, 46.6, 47.2, 53.7, 61.5, 65.9, 69.4, 71.3, 168.8, 169.3, 170.4, 170.5, 170.9, 171.1, 171.4, 173.0, 173.3. IR ($CHCl_3$, cm^{-1}): 3296, 3079, 2920, 2851, 1743, 1658, 1652, 1547, 1467, 1411, 1378, 1341, 1203, 1132, 1031. HRMS (FAB): Calcd for $C_{68}H_{128}N_9O_{11}$ $[M - CF_3COO]^+$, 1246.9733; found, 1246.9696.

Preparation of $(C_{18}H_{37})_2NCOCH_2OCH_2CO$-$(Gly)_3$-Pro-Gln-Ala-Gly-$OC_7H_{15}$, 5

L-Glycine heptyl ester tosylate. A solution of glycine (2.00 g, 26.7 mmol), TsOH monohydrate (5.70 g, 30.0 mmol) and 1-heptanol (15 mL, 106 mmol) in toluene (18 mL) was refluxed for 12 h. Water was removed from the reaction mixture by using a Dean–Stark adapter. The reaction mixture was cooled to room temperature, diethyl ether added (50 mL) and the mixture cooled at 0 °C for 2 h. The solid was collected and recrystallized from methanol–ether to afford white crystals (4.91 g, 53%), mp 105–106 °C. ^{1}H-NMR: 0.87 (3H, t, J = 6.9 Hz, CH_2CH_3), 1.23 (8H, pseudo-s, $OCH_2CH_2(CH_2)_4CH_3$), 1.49 (2H, quintet, J = 6.8 Hz, $OCH_2CH_2(CH_2)_4CH_3$), 2.33 (3H, s, $CH_3C_6H_4SO_3$), 3.65 (2H, q, J = 5.8 Hz, NH_3CH_2CO), 3.99 (2H, t, J = 6.9 Hz, $OCH_2CH_2(CH_2)_4CH_3$), 7.10 (2H, d, J = 7.8 Hz, Tosyl H_{Ar}), 7.72 (2H, d, J = 7.8 Hz, Tosyl H_{Ar}), 8.03 (3H, bt, NH_3CH_2CO). ^{13}C-NMR: 14.0, 21.3, 22.6, 25.6, 28.2, 28.9, 31.7, 40.3, 66.3, 126.0, 128.9, 140.4, 141.2, 167.4. IR ($CHCl_3$, cm^{-1}): 3473, 3030, 2961, 2929, 2856, 2730, 2643, 2220, 1996, 1911, 1747, 1616, 1600, 1519, 1471, 1428, 1380, 1194, 1127, 1105, 1056, 1036, 1012.

Boc-AG-OC_7H_{15}. TsOH·G-OC_7H_{15} (0.51 g, 1.49 mmol), Boc-L-Ala (0.28 g, 1.48 mmol), EDCI (0.31 g, 1.62 mmol) and HOBt (0.22 g, 1.63 mmol) were dissolved in CH_2Cl_2 (40 mL). Et_3N (0.61 mL) was then added. The mixture was stirred at 0 °C for 0.5 h and then at room temperature for 48 h. The solvent was evaporated and the residue was dissolved in CH_2Cl_2 (40 mL) and washed with 5% citric acid (2 × 20 ml), H_2O (2 × 20 mL), 5% $NaHCO_3$ (2 × 20 mL) and brine (2 × 20 mL), dried over $MgSO_4$ and evaporated. The residue was purified by column chromatography (silica gel, EtOAc : hexane = 40 : 60) to give an oil (0.42 g, 83%). ^{1}H-NMR: 0.87 (3H, t, J = 6.3 Hz, CH_2CH_3), 1.20–1.35 (8H, m, $OCH_2CH_2(CH_2)_4CH_3$), 1.37 (3H, d, J = 7.2 Hz, Ala CH_3), 1.44 (9H, s, $C(CH_3)_3$), 1.63 (2H, quintet, J = 6.6 Hz, $OCH_2CH_2(CH_2)_4CH_3$), 4.02 (2H, d, J = 5.1 Hz, Gly CH_2), 4.13 (2H, t, J = 6.8 Hz, $OCH_2CH_2(CH_2)_4CH_3$), 4.23 (1H, broad quintet, Ala *CH*), 5.11 (1H, d, J = 6.6 Hz, Ala *NH*), 6.79 (1H, bs, Gly *NH*). ^{13}C-NMR: 14.2, 18.5, 22.8, 26.0, 28.5, 28.7, 29.0, 31.9, 41.5, 65.9, 80.5, 100.2, 170.0, 173.0. IR ($CHCl_3$, cm^{-1}): 3320, 3088, 2958, 2932, 2859, 1753, 1715, 1668, 1531, 1455, 1392, 1367, 1291, 1250, 1172, 1068, 1048, 1028.

Boc-QAG-OC_7H_{15}. Boc-AG-OC_7H_{15} was deprotected in the usual way (4 N HCl in dioxane for 1 h). HCl·AG-OC_7H_{15} (0.48 g, 1.71 mmol), Boc-Gln-OH (0.42 g, 1.71 mmol), EDCI (0.36 g, 1.88 mmol) and HOBt (0.25 g, 1.88 mmol) were dissolved in CH_2Cl_2 (35 mL). The mixture was stirred at 0 °C for 0.5 h and then at room temperature for 12 h. The residue was dissolved in CH_2Cl_2 (35 mL), washed with 5% citric acid (2 × 25 mL), H_2O (2 × 25 mL), 5% $NaHCO_3$ (2 × 25 mL) and brine (25 mL), dried over $MgSO_4$ and evaporated. Column chromatography (silica gel, $CHCl_3$: CH_3OH = 97 : 3) afforded a solid (0.54 g, 67%). ^{1}H-NMR: 0.88 (3H, t, J = 6.6 Hz, CH_2CH_3), 1.20–1.38 (8H, m, $OCH_2CH_2(CH_2)_4CH_3$), 1.40–1.49 (12H, m, Ala CH_3 and $C(CH_3)_3$), 1.63 (2H, quintet, J = 6.3 Hz, $OCH_2CH_2(CH_2)_4CH_3$), 1.98–2.15 (2H, m, Gln CH_2CH_2CO), 2.40 (2H, t, J = 6.2 Hz, Gln CH_2CH_2CO), 3.91–4.03 (2H, m, Gly CH_2), 4.11 (2H, t, J = 6.8 Hz, $OCH_2CH_2(CH_2)_4CH_3$), 4.24 (1H, bs, Gln *CH*), 4.55 (1H, quintet, J = 7.2 Hz, Ala *CH*), 5.79 (1H, bs, Gln $CONH_2$), 6.40 (1H, bs, Gln $CONH_2$), 7.02 (1H, bs, Gln *NH*), 7.30 (1H, bt, Gly *NH*), 7.68 (1H, bd, Ala *NH*). ^{13}C-NMR: 14.2, 17.8, 22.7, 26.0, 28.5, 28.7, 29.0, 29.1, 31.9, 41.5, 49.3, 53.9, 65.9, 80.5, 170.3, 172.1, 173.0, 176.1. IR ($CHCl_3$, cm^{-1}): 3433, 3318, 3076, 2959, 2930, 2857, 1735, 1688, 1644, 1527, 1451, 1392, 1366, 1346, 1287, 1271, 1246, 1172, 1052, 1028, 872, 780, 665.

Boc-PQAG-OC_7H_{15}. Boc-QAG-OC_7H_{15} was deprotected in 4 N HCl in dioxane for 1 h. HCl·QAG-OC_7H_{15} (0.37 g, 0.91 mmol), Boc-Pro-OH (0.20 g, 0.91 mmol), EDCI (0.19 g, 1.00 mmol) and HOBt (0.14 g, 1.00 mmol) were dissolved in CH_2Cl_2 (35 mL). Et_3N (0.38 mL) was added and the mixture was stirred at 0 °C for 0.5 h and then at rt for 12 h. The residue was dissolved in CH_2Cl_2 (35 mL), washed with 5% citric acid (2 × 25 mL), H_2O (2 × 25 mL), 5% $NaHCO_3$ (2 × 25 mL) and brine (25 mL), dried over $MgSO_4$, and evaporated. The residue was purified by column chromatography (silica gel, $CHCl_3$: CH_3OH 95 : 5) to give a white solid (0.41 g, 79%). ^{1}H-NMR: 0.88 (3H, t, J = 6.6 Hz, CH_2CH_3), 1.20–1.37 (8H, m, $OCH_2CH_2(CH_2)_4CH_3$), 1.40–1.50 (12H, m, Ala CH_3 and $C(CH_3)_3$), 1.62 (2H, quintet, J = 6.9 Hz, $OCH_2CH_2(CH_2)_4CH_3$), 1.83–2.48 (8H, m, Pro $NCH_2CH_2CH_2$ and Gln CH_2CH_2CO), 3.39–3.49 (1H, m, Pro $NCH_2CH_2CH_2$), 3.64–3.74 (1H, m, Pro $NCH_2CH_2CH_2$), 3.88–4.04 (2H, m, Gly CH_2), 4.10 (2H, t, J = 6.8 Hz, $OCH_2CH_2(CH_2)_4CH_3$), 4.18 (1H, dd, J = 8.6, 4.6 Hz, Pro *CH*), 4.27 (1H, q, J = 5.7 Hz, Gln *CH*), 4.46 (1H, quintet, J = 7.5 Hz, Ala *CH*), 5.68 (1H, bs, Gln $CONH_2$), 6.55 (1H, bs, Gln $CONH_2$), 7.40 (1H, t, J = 5.4 Hz, Gly *NH*), 8.02 (1H, d, J = 7.2 Hz, Ala *NH*), 8.78 (1H, bd, Gln *NH*). ^{13}C-NMR: 14.2, 17.5, 22.8, 24.9, 26.0, 28.6, 28.7, 29.1, 30.3, 31.6, 31.9, 41.5, 47.4, 49.9, 55.0, 57.0, 61.7, 65.5, 81.0, 165.6, 170.0, 171.6, 174.8, 176.6, 179.3. IR ($CHCl_3$, cm^{-1}): 3409, 3296, 3079, 2959, 2930, 2858, 1744, 1698, 1662, 1634, 1547, 1454, 1406, 1366, 1286, 1211, 1163, 1123, 1091, 978, 771, 666.

18_2DGA-GGGPQAG-OC_7H_{15}, 5. Boc-PQAG-OC_7H_{15} was deprotected by using 4 N HCl in dioxane for 1 h. 18_2DGA-GGG-OH (0.40 g, 0.46 mmol), HCl·PQAG-OC_7H_{15} (0.24 g, 0.46 mmol), EDCI (0.10 g, 0.50 mmol) and HOBt (0.07 g, 0.50 mmol) were suspended in CH_2Cl_2 (30 mL). To this mixture Et_3N (0.19 mL) was added. The mixture was stirred at 0 °C for 0.5 h and then at rt for 48 h. The solvent was evaporated *in vacuo* and the residue was crystallized from MeOH. The crude product was chromatographed (silica gel, $CHCl_3$: CH_3OH : HOAc 90 : 10 :

0.1) to afford a solid (0.18 g, 31%). ^{1}H-NMR: 0.88 (3H, t, J = 6.4 Hz, CH_2CH_3), 1.26 (68H, *pseudo*-s, $CH_3(CH_2)_{15}CH_2CH_2N$ and $OCH_2CH_2(CH_2)_4CH_3$), 1.45–1.66 (9H, m, Ala CH_3, $CH_3(CH_2)_{15}CH_2CH_2N$ and $OCH_2CH_2(CH_2)_4CH_3$), 1.98–2.53 (8H, m, Pro $NCH_2CH_2CH_2$ and Gln CH_2CH_2CO), 3.09 (2H, t, J = 7.2 Hz, $CH_3(CH_2)_{15}CH_2CH_2N$), 3.28 (2H, t, J = 7.4 Hz, $CH_3(CH_2)_{15}CH_2CH_2N$), 3.45–3.55 (2H, m, Pro $NCH_2CH_2CH_2$), 3.78–4.18 (13H, m, four Gly CH_2, $OCH_2CH_2(CH_2)_4CH_3$, $COCH_2O$ and Pro *CH*), 4.32 (2H, s, $COCH_2O$), 4.40–4.54 (2H, m, Gln *CH* and Ala *CH*), 6.48 (1H, bs, Gln $CONH_2$), 7.12 (1H, bs, Gln $CONH_2$), 7.50–7.60 (2H, m, two Gly *NH*), 7.68 (1H, d, J = 7.5 Hz, Ala *NH*), 7.99 (1H, bt, Gly *NH*), 8.42 (1H, bt, Gly *NH*), 8.84 (1H, bd, Gln *NH*). ^{13}C-NMR: 14.3, 17.6, 22.8, 22.9, 25.2, 26.0, 27.1, 27.3, 27.8, 28.7, 29.0, 29.1, 29.5, 29.6, 29.8, 29.9, 31.9, 32.1, 41.4, 42.4, 43.3, 46.7, 47.2, 49.7, 54.1, 61.8, 65.6, 69.5, 71.6, 168.8, 169.3, 170.1, 170.3, 170.4, 171.3, 171.4, 173.0, 173.6, 177.4. IR ($CHCl_3$, cm^{-1}): 3302, 3077, 2923, 2854, 1747, 1660, 1544, 1466, 1378, 1260, 1201, 1130, 1028. Anal. calcd for $C_{68}H_{125}N_9O_{12}$: C, 64.78; H, 9.99; N, 10.00%. Found: C, 64.80; H, 9.86; N, 10.11%.

Preparation of $(C_{18}H_{37})_2NCOCH_2OCH_2CO$-(Gly)$_3$-Pro-Lys(ε-N-Boc)-(Gly)$_2$-$OC_7H_{15}$, 3 and $(C_{18}H_{37})_2NCOCH_2OCH_2CO$-(Gly)$_3$-Pro-Lys(ε-N-dansyl)-(Gly)$_2$-OC_7H_{15}, 4

Preparation of **3** and **4** have been reported previously.[35]

Vesicle preparation and chloride release measurement

Phospholipid vesicles from 7 : 3 1,2-dioleyl-*sn*-glycero-3-phosphocholine (DOPC) and 1,2-dioleyl-*sn*-glycero-3-phosphate monosodium salt (DOPA, both from Avanti Polar Lipids) or DOPC were prepared in the presence of an internal, chloride containing buffer (600 mM KCl, 10 mM HEPES, adjusted to pH = 7). After extrusion through a 200 nm filter and exchange of external solution with a chloride-free buffer (400 mM K_2SO_4, 10 mM HEPES, adjusted to pH = 7), vesicles were suspended in the same external buffer (final phospholipid concentration about 0.31 mM). An approximate vesicle size of 200 nm was confirmed by using a particle analyzer. The electrode was introduced into the solution and allowed to equilibrate. The voltage output was recorded and after the baseline became flat, aliquots of the solution of compound at study (9 mM in isopropanol) were added. Complete lysis of the vesicles was induced by addition of a 2% aqueous solution of Triton X100 (100 μL) and the data collected were normalized to this value. The data were collected by Axoscope 9.0 using a DigiData 1322A series interface.

Fluorescence spectroscopy

Fluorescence was recorded by using a Perkin Elmer LS50B fluorimeter on continuously stirred samples. A stock solution (0.50 mM **4** in 2-PrOH) was prepared. Compound was added and stirred for about 60 s before spectra were recorded. Except as indicated, the emission spectrum was measured in 2 mL external buffer (400 mM K_2SO_4, 10 mM HEPES, pH 7.0). For solvent dependence experiments, 2 mL freshly distilled solvent instead of buffer was used and the concentration was adjusted for the instrument capacity. For the measurement in the vesicles, compound was added to the liposome suspension (as prepared above, in 2 mL external buffer) and the overall lipid concentration was 0.31 mM (same as chloride release experiment). The excitation wavelength was 340 nm and the emission spectrum was recorded between 300–600 nm (2.5 nm slit width, 400 nm min^{-1} scan speed, average three scans).

Computational method

All calculations were performed using the Gaussian 03 suite of computer programs. Geometry optimization and frequency analysis were done by using density functional theory method (B3LYP/6–31G*). All geometries were completely optimized in the gas phase; the structures reported here are true minima on the potential energy surfaces. This was confirmed by vibration calculations without imaginary vibrational frequencies. For those complexes which have multiple-conformations, several conformations have been calculated and the ones with lowest energy were selected for the final structure.

Acknowledgements

We thank the NIH for grants (GM 36262, GM 63190) for support of this work.

References

1 R. B. Gennis, *Biomembranes: Molecular Structure and Function*, Springer Verlag, New York, 1989, p. 533.
2 P. Yeagle, *The structure of biological membranes*, CRC Press, Boca Raton, 1992,p. 1227.
3 *Membrane Dynamics and Domains*, ed. P. J. Quinn, Kluwer Academic/Plenum Publishers, New York, 2004; vol. 37, p. 499.
4 J. M. Sanderson and E. J. Whelan, *Phys. Chem. Chem. Phys.*, 2004, **6**, 1012–1017.
5 M. E. Weber, E. K. Elliott and G. W. Gokel, *Org. Biomol. Chem.*, 2006, **4**, 83–89.
6 *Lipid Bilayers: Structure and Interactions*, ed. J. Katsaras and T. Gutberlet, Springer Verlag, Berlin, 2001, p. 295.
7 J. Andra, D. Monreal, G. Martinez de Tejada, C. Olak, G. Brezesinski, S. S. Gomez, T. Goldmann, R. Bartels, K. Brandenburg and I. Moriyon, *J. Biol. Chem.*, 2007, **282**, 14719–14728.
8 P. Li, M. Sun, T. Wohland, D. Yang, B. Ho and J. L. Ding, *Biochemistry*, 2006, **45**, 10554–10562.
9 D. Gidalevitz, Y. Ishitsuka, A. S. Muresan, O. Konovalov, A. J. Waring, R. I. Lehrer and K. Y. Lee, *Proc. Natl. Acad. Sci. U. S. A.*, 2003, **100**, 6302–6307.
10 S. Fernandez-Lopez, H.-S. Kim, E. C. Choi, M. Delgado, J. R. Granja, A. Khasanov, K. Kraehenbuehl, G. Long, D. A. Weinberger, K. M. Wilcoxen and M. R. Ghadiri, *Nature*, 2001, **412**, 452–455.
11 N. A. Lockwood, J. R. Haseman, M. V. Tirrell and K. H. Mayo, *Biochem. J.*, 2004, **378**, 93–103.
12 M. Ouellet, G. Bernard, N. Voyer and M. Auger, *Biophys. J.*, 2006, **90**, 4071–4084.
13 G. Das and S. Matile, *Proc. Natl. Acad. Sci. U. S. A.*, 2002, **99**, 5183–5188.
14 W. M. Leevy, G. M. Donato, R. Ferdani, W. E. Goldman, P. H. Schlesinger and G. W. Gokel, *J. Am. Chem. Soc.*, 2002, **124**, 9022–9023.
15 A. L. Sisson, M. R. Shah, S. Bhosale and S. Matile, *Chem. Soc. Rev.*, 2006, **35**, 1269–1286.
16 A. P. Davis, D. N. Sheppard and B. D. Smith, *Chem. Soc. Rev.*, 2007, **36**, 348–357.
17 T. M. Fyles, *Chem. Soc. Rev.*, 2007, **36**, 335–347.
18 B. A. McNally, W. M. Leevy and B. D. Smith, *Supramol. Chem.*, 2007, **19**, 29–37.
19 (*a*) P. V. Santacroce, J. T. Davis, M. E. Light, P. A. Gale, J. C. Iglesias-Sanchez, P. Prados and R. Quesada, *J. Am. Chem. Soc.*, 2007, **129**, 1886–1887; (*b*) P. A. Gale, J. Garric, M. E. Light, B. A. McNally and B. D. Smith, *Chem. Commun.*, 2007, 1736–1738; (*c*) X. Li, B. Shen, X. Q. Yao and D. Yang, *J. Am. Chem. Soc.*, 2007, **129**, 7264–7265.

20 P. H. Schlesinger, R. Ferdani, J. Liu, J. Pajewska, R. Pajewski, M. Saito, H. Shabany and G. W. Gokel, *J. Am. Chem. Soc.*, 2002, **124**, 1848–1849.
21 R. Pajewski, R. Garcia-Medina, S. L. Brody, P. H. Schlesinger and G. W. Gokel, *Chem. Commun.*, 2006, 329–331.
22 N. Djedovic, R. Ferdani, E. Harder, J. Pajewska, R. Pajewski, M. E. Weber, P. H. Schlesinger and G. W. Gokel, *New J. Chem.*, 2005, **29**, 291–305.
23 R. Ferdani and G. W. Gokel, *Org. Biomol. Chem.*, 2006, **4**, 3746–3750.
24 L. You, R. Ferdani and G. W. Gokel, *Chem. Commun.*, 2006, 603–605.
25 L. You, R. Ferdani, R. Li, J. P. Kramer, R. E. K. Winter and G. W. Gokel, *Chem.–Eur. J.*, 2008, **14**, 382–396.
26 R. Dutzler, E. B. Campbell and R. MacKinnon, *Science*, 2003, **300**, 108–112.
27 R. Dutzler, *Curr. Opin. Struct. Biol.*, 2006, **16**, 439–446.
28 R. Ferdani, R. Pajewski, J. Pajewska, P. H. Schlesinger and G. W. Gokel, *Chem. Commun.*, 2006, 439–441.
29 C. Reichardt, *Solvents, and solvent effects in organic chemistry*, Wiley-VCH Verlag GmbH, Weinheim, 3rd edn, 2003, p. 629.
30 R. G. Hanshaw, R. V. Stahelin and B. D. Smith, *Chem.–Eur. J.*, 2008, **14**, 1690–1697.
31 N. Madhavan and M. S. Gin, *ChemBioChem*, 2007, **8**, 1834–1840.
32 R. Pajewski, R. Ferdani, J. Pajewska, R. Li and G. W. Gokel, *J. Am. Chem. Soc.*, 2005, **126**, 18281–18295.
33 G. A. Cook, R. Pajewski, M. Aburi, P. E. Smith, O. Prakash, J. M. Tomich and G. W. Gokel, *J. Am. Chem. Soc.*, 2006, **128**, 1633–1638.
34 (*a*) M. S. P. Sansom, *Curr. Opin. Struct. Biol.*, 1998, **8**, 237–244; (*b*) C. Chipot, M. L. Klein and M. Tarek, *Handbook of Materials Modeling*, Springer, Dordrecht, Netherlands, 2005, pp. 929–958; (*c*) Z. Donko, P. Hartmann, G. J. Kalman and K. I. Golden, *J. Phys. A: Math. Gen.*, 2003, **36**, 5877–5885.
35 L. You and G. W. Gokel, *Chem.–Eur. J.*, 2008, DOI: 10.1002/chem.200800147.